INSTITUTE OF PHYSICS PUBLISHING JOURNAL OF PHYSICS: CONDENSED MATTER

J. Phys.: Condens. Matter **19** (2007) 065146 (12pp) doi:10.1088/0953-8984/19/6/065146

Diffusion and reaction in crowded environments

Carlos Echeverría[1,2], **Kay Tucci**[2,3] **and Raymond Kapral**[4]

[1] Laboratorio de Física Aplicada y Computacional, Departamento de Matemática y Física, Universidad Nacional Experimental del Táchira, San Cristobal 5001, Venezuela
[2] Centro de Física Fundamental, Universidad de Los Andes, Mérida 5101, Venezuela
[3] SUMA-CeSiMo, Universidad de Los Andes, Mérida 5101, Venezuela
[4] Chemical Physics Theory Group, Department of Chemistry, University of Toronto, Toronto, ON, M5S 3H6, Canada

E-mail: cecheve@ula.ve, kay@ula.ve and rkapral@chem.utoronto.ca

Received 8 September 2006
Published 22 January 2007
Online at stacks.iop.org/JPhysCM/19/065146

Abstract

The effects of molecular crowding on small molecule diffusion and chemical reaction rate coefficients are investigated. The systems considered comprise a random distribution of stationary spherical obstacles occupying a volume fraction ϕ of the system and a large number of small molecules whose dynamics are followed. Chemical reactions are studied in such crowded systems where, in addition to the obstacles, a large reactive sphere C is present that catalyses the reaction $A + C \rightarrow B + C$. Using a mesoscopic description of the dynamics employing multiparticle collisions among the small molecules, the ϕ dependence of the diffusion and reaction rate coefficients is computed. Both the diffusion and reaction rate coefficients decrease with increase of the obstacle volume fraction as expected but variations of these quantities with ϕ are not predicted by simple models of the dynamics.

1. Introduction

Diffusion and reaction are two of the most basic transport mechanisms that underlie the description of a wide range of chemical and biological processes. Numerous investigations have been devoted to the measurement and computation of diffusion and rate coefficients in bulk homogeneous solutions. These transport processes can be modified significantly when the environment is crowded by a high density of obstacles. An important example of a crowded molecular system is a biological cell.

The environment of the living cell is very different from that usually encountered in laboratory studies of chemical reactions [1]. The cellular volume is occupied by structural elements such as microtubules and filaments, various organelles and a variety of other macromolecular species. Such environments are called crowded since no one species may be in high concentration but collectively the macromolecular species occupy a large volume fraction

of the cell, typically ranging from 0.1 to 0.4 of the total cellular volume [2, 3]. Crowding is used to refer to the effects of steric repulsions on reactive and diffusion processes that take place in media with a high volume fraction of obstacles.

The effects of crowding in cellular environments have been recognized and studied for many years [4–6]. Crowding can influence the equilibrium properties of the system such as equilibrium constants (or even transition state theory estimates of rate constants) by changing the activities of chemical species. Crowding can also change transport properties. It is well established that crowding can considerably decrease the diffusion coefficients of macromolecules [7, 8], influence diffusion-controlled reaction rates [9], lead to shifts in chemical equilibria [10], alter protein folding processes and influence protein assembly [11–15]. The largest effects are seen for macromolecules but crowding also influences the dynamics of small molecules.

In this paper we study effects of crowding on the dynamical properties of small molecules. While our investigations are motivated by effects seen in crowded cellular environments, we make no attempt to realistically model the internal structure of a crowded biological cell. Instead, we consider a simple model where small particles undergo motion among a random distribution of stationary spherical obstacles and compute the volume fraction dependence of the diffusion coefficient. We also study the situation where a large catalytic sphere is present in the sea of obstacles. The large sphere catalyses the conversion of a species A to a species B and we compute the reaction rate coefficient as a function of the volume fraction of obstacles. Since it is difficult to obtain analytical estimates for these transport properties for arbitrary values of the volume fraction, our results are obtained from simulations of the dynamics using a mesoscopic model that retains the essential conservation laws of full molecular dynamics [16–18]. Thus, while our model is simple, it does capture some of the generic features of crowding effects on small molecule motion and forms the starting point for the construction of more detailed models of crowded cellular environments.

In section 2 we give the details of the model and describe the multiparticle collision dynamics that is employed in the simulations. Diffusion of small particles in a field of obstacles in considered in section 3 and the simulation results are compared with analytical estimates of the volume fraction dependence of the diffusion coefficient. In section 4 we describe how the reaction rate can be computed for diffusion-influenced reactions occurring in a field of inert obstacles. The conclusions of the study are given in section 5.

2. Mesoscopic dynamics in crowded environments

The simulations of diffusion and reaction in crowded environments were carried out on a model system comprising a large number of particles undergoing reactive and non-reactive dynamics in a field of spherical obstacles. More specifically, we consider a three-dimensional system with volume V containing numbers N_A and N_B ($N = N_A + N_B$) of A and B type point particles with mass m. The volume contains a single stationary catalytic sphere C with radius σ_C on whose surface the irreversible reaction $A + C \rightarrow B + C$ takes place. In addition, the volume contains a number N_S of other stationary spherical obstacles with radius σ. The volume fraction of obstacles and catalytic particle is $\phi = 4\pi(N_S\sigma^3 + \sigma_C^3)/3V \equiv \phi_o + \phi_C$, where ϕ_o and ϕ_C are the volume fractions of obstacles and catalytic spheres, respectively. Periodic boundary conditions were employed in the simulations.

In order to simplify the dynamical description while retaining the essential features of full molecular dynamics (MD), we describe the evolution of the A and B particles using multiparticle collision (MPC) dynamics (also called stochastic rotation dynamics) [16–18]. In MPC dynamics particles with continuous positions and velocities free stream between

multiparticle collision events that occur at discrete times τ. To carry out collisions, the volume V is divided into cubic cells with length ℓ labelled by an index ξ. At every time τ each cell is assigned at random a rotation operator $\hat{\omega}_\xi$, chosen from some set of rotation operators. If N_ξ is the instantaneous number of particles in cell ξ, the centre of mass velocity in the cell is $\mathbf{V}_\xi = N_\xi^{-1} \sum_{i=1}^{N_\xi} \mathbf{v}_i$ where $\mathbf{v}_i$ is the velocity of particle i. In MPC dynamics the post-collision velocity is given by

$$\mathbf{v}_i' = \mathbf{V}_\xi + \hat{\omega}_\xi(\mathbf{v}_i - \mathbf{V}_\xi). \tag{1}$$

It has been shown that this mesoscopic dynamics preserves mass, momentum and energy and the single-particle velocity distribution is Maxwellian [16]. It also yields the full set of hydrodynamic equations on long distance and timescales and the transport properties of the model can be computed [16–22]. Thus, it provides a simple mesoscopic description of the dynamics that retains the important features of MD yet allows large scale simulations of the dynamics to be carried out for long times. MPC dynamics has been used previously to study friction and hydrodynamic interactions [23, 24], polymer dynamics [25–32], suspensions [33–35] and reaction–diffusion systems [36, 37]. In general we may choose different kinds of MPC dynamics for the different species [36] but for simplicity here the A and B species are assumed to undergo identical MPC collisions.

The obstacles are taken to be hard spherical objects. When an A or B particle collides with an obstacle its velocity is reversed (bounce-back collisions). The catalytic particle C is special. It too is a hard spherical object but when an A particle collides with its surface not only is its velocity reversed but with probability p_R it is converted to a B-type particle. For the irreversible reactive case we consider here, the identities of the B particles are not changed when they collide with C.

The simulations presented in this paper were carried out on systems with volume $V = (50)^3$ or $V = (100)^3$ multiparticle collision cells with unit volume. The rotation operators in the MPC dynamics were taken to describe rotations by $\pm\pi/2$ about randomly chosen axes. The catalytic sphere with radius $\sigma_C = 10$ was placed in the centre of the simulation volume. The number of obstacles with radius $\sigma = 1$ was computed from the desired value of the volume fraction ϕ and obstacles were randomly placed in the volume, ensuring that there were neither overlaps among the obstacles nor with the catalytic sphere. The total mean density of A and B particles with unit mass was taken to be $n_0 = 5$ particles per cell. The temperature in reduced units ($m = 1$, $\ell = 1$, $\tau = 1$) was $T = 1/3$. Thus, a particle moving with a velocity corresponding to the mean thermal velocity will travel a distance of one cell between multiparticle collisions. For parameter regimes where the particles travel on average a small fraction of a cell, random multiparticle collision grid shifting can be introduced to restore Galilean invariance [19].

3. Diffusion in a field of obstacles

Before investigating chemically reacting systems, we consider diffusion of the small A or B particles in a random field of stationary obstacles with $\sigma = 1$ and a volume fraction $\phi_o = 4\pi N_S \sigma^3/3V \equiv \phi$. The catalytic sphere is not present in the system. Our interest is in $D(\phi)$, the diffusion coefficient as a function of the volume fraction. In the absence of obstacles it is not difficult to compute an approximate analytical expression for the diffusion coefficient D_0 for multiparticle collision dynamics. The result is [36]

$$D_0 = \frac{k_B T}{2m}\left(\frac{2n_0 + 1 - e^{-n_0}}{n_0 - 1 + e^{-n_0}}\right), \tag{2}$$

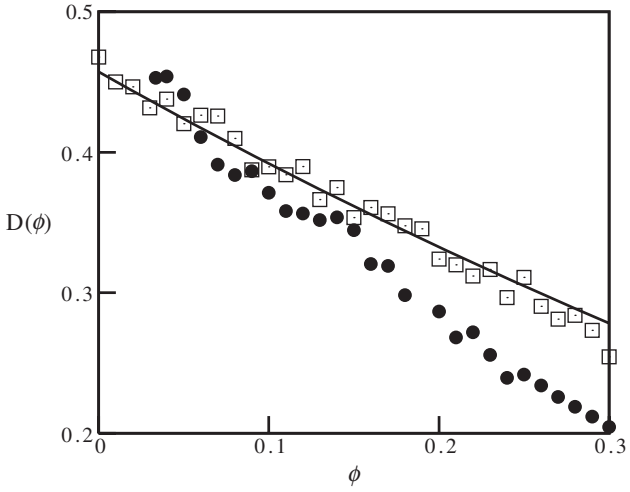

Figure 1. Diffusion coefficient $D(\phi)$ (squares) as a function of the volume fraction ϕ. The solid line is the theoretical estimate given in equation (4). The solid circles are the results of simulations of $D(\phi)$ when the catalytic sphere is present.

where n_0 is the total density of the small particles. Comparison of this formula with the results of simulations has shown that this analytical expression provides an accurate estimate of the diffusion coefficient [36]. In the presence of obstacles, we expect the diffusion coefficient to decrease and this is indeed the case as figure 1 shows. The diffusion coefficient was computed from the mean square displacement of the small particles. Since the A and B particles are mechanically identical, we need not distinguish these species in the computation of the self-diffusion coefficient.

If we assume that $n(\mathbf{r}, t)$, the total density field of the A and B particles outside the obstacles, obeys the diffusion equation and the obstacles are accounted for by an induced diffusion flux field $\mathbf{J}(\mathbf{r}, t)$, the evolution equation for the density field is

$$\frac{\partial}{\partial t} n(\mathbf{r}, t) = D_0 \nabla^2 n(\mathbf{r}, t) - \nabla \cdot \mathbf{J}(\mathbf{r}, t). \tag{3}$$

Starting from this equation, it is possible to derive an equation for $\langle n(\mathbf{r}, t)\rangle$, the density field averaged over the configuration of the obstacles, which yields an effective volume fraction dependent expression for the diffusion coefficient. In the mean field limit, assuming a random distribution of obstacles, the result is [38]

$$D(\phi) = D_0 \frac{1-\phi}{1+\phi/2}. \tag{4}$$

The solid line in figure 1 is a plot of this function and is seen to be in good agreement with the simulation results.

Next, we compute the diffusion coefficient for a system containing a large catalytic sphere with radius $\sigma_C = 10$ and a distribution of obstacles with $\sigma = 1$. A picture of the catalytic sphere and a configuration of the obstacles for $\phi = 0.15$ is shown in figure 2. The plot of $D(\phi)$ for this case in figure 1 (solid circles) indicates that the diffusion coefficient of the A or B particles decreases more strongly with increase in the volume fraction than when the large catalytic sphere is absent. In our model the chemical reaction is a simple relabelling process from A to B with probability p_R upon collision with the catalytic sphere. Since the A and B particles are mechanically identical the diffusive motion is independent of the species label.

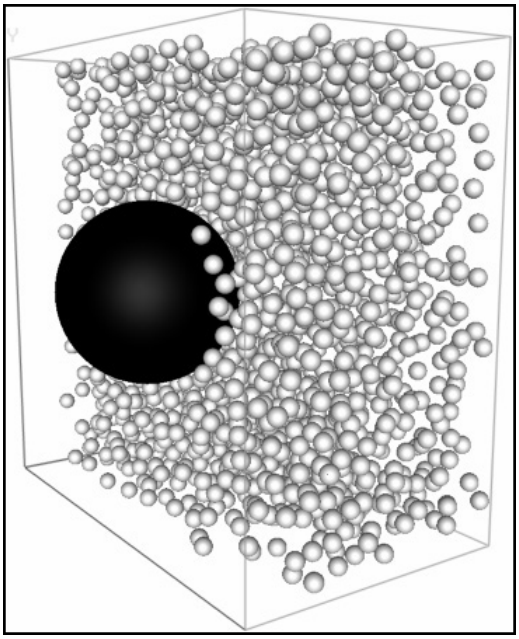

Figure 2. The large catalytic sphere (black) surrounded by obstacle spheres (light grey) for a volume fraction $\phi = 0.15$. Obstacle spheres in half of the volume are shown in order to see the embedded catalytic sphere. None of the small A or B molecules are shown. They fill the interstices between the obstacles.

Consequently, any change in the diffusion coefficient must be attributed to the configuration and volume fraction of obstacles with the catalytic sphere present.

Our simulations were carried out using periodic boundary conditions; therefore, the finite-size systems we study consist of a periodic array of catalytic spheres whose volume fraction is ϕ_C. An approximate analytical expression for the diffusion coefficient, $D^C(\phi_C)$, of small molecules in a cubic array of spherical scatterers has been determined [38]. The result has the same general form as that given in equation (4) with the catalytic sphere volume fraction ϕ_C replacing ϕ. This expression was derived under the assumption that the dynamics of the small molecules is described a simple diffusion equation where no obstacles are present. In our system, the spaces between the catalytic spheres are filled with obstacles and small diffusing molecules. The effect of the obstacles can be accounted for by replacing D_0 by the full expression for $D(\phi_o)$ in equation (4), the diffusion coefficient in the presence of obstacles with volume fraction ϕ_o, but without a catalytic sphere. Thus, the approximate expression for the diffusion coefficient $D^C(\phi)$ is

$$D^C(\phi) = D(\phi - \phi_C)\frac{1-\phi_C}{1+\phi_C/2} = D_0\frac{1-\phi+\phi_C}{1+\phi/2-\phi_C/2}\frac{1-\phi_C}{1+\phi_C/2}, \tag{5}$$

where we used the fact that $\phi_o = \phi - \phi_C$. For the simulation conditions in figure 1 ϕ_C is very small ($\phi_C \approx 0.0335$) and equation (5) is not able to describe the simulation results. However, the presence of a large catalytic sphere can lead to structural ordering of the obstacles in its vicinity and we now investigate this effect.

Figure 3 shows the local volume fraction $\phi(r)$ as a function of the distance from the centre of the catalytic sphere for several values of the global obstacle volume fraction. As the global volume fraction of obstacles increases strong deviations from uniformity appear giving rise to

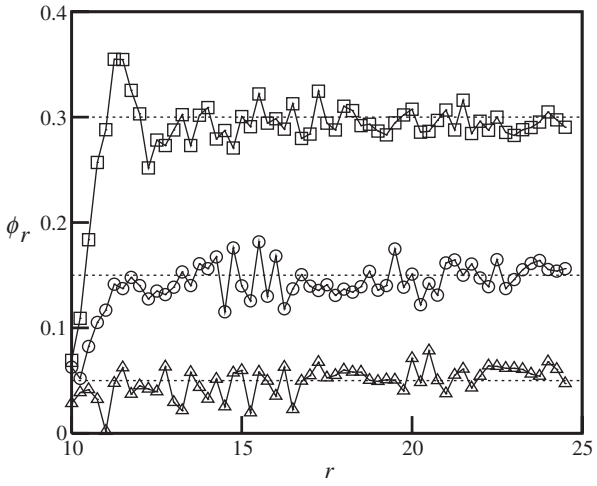

Figure 3. Local volume fraction, $\phi(r)$, as a function of the distance, r, to the centre of the catalytic sphere. Squares circles and triangles represent the volume fraction for systems with $\phi = 0.30$, 0.15, and 0.05, respectively.

structural ordering near the catalytic sphere signalled by a peak in $\phi(r)$. As a consequence of this structure, there is an increased local density of small particles in the vicinity of the catalytic sphere surface and they remain trapped for longer periods of time for large values of the obstacle volume fraction. This effect is not captured by the analytical model which assumes a random distribution of obstacles.

4. Reactive dynamics in a field of obstacles

We now describe how the chemical reaction rate coefficient for the irreversible reaction $A+C \rightarrow B+C$ which occurs when A particles encounter the catalytic sphere can be calculated. The time dependent rate coefficient $k_f(t)$ for this reaction can be defined by the rate law,

$$\frac{\mathrm{d}}{\mathrm{d}t}\bar{n}_A(t) = -k_f(t)n_C\bar{n}_A(t), \tag{6}$$

where $\bar{n}_A(t)$ is the mean number density of species A at time t. For long times the rate coefficient tends to the rate constant $k_f = \lim_{t\rightarrow\infty} k_f(t)$.

For a single catalytic sphere (or a dilute suspension of catalytic spheres with number density n_C) the result for $k_f(t)$ is well known if the field of A and B particles is described by the diffusion equation,

$$\frac{\partial n_A(\mathbf{r},t)}{\partial t} = D_A\nabla^2 n_A(\mathbf{r},t). \tag{7}$$

The problem was solved by Smoluchowski [39, 40] for complete absorption of the A particles on the catalytic sphere surface and by Collins and Kimball [41] for the 'radiation' boundary condition,

$$4\pi D\bar{\sigma}^2\hat{\mathbf{r}}\cdot(\nabla n_A)(\hat{\mathbf{r}}\bar{\sigma}_C,t) = k_{0f}n_A(\hat{\mathbf{r}}\bar{\sigma}_C,t). \tag{8}$$

This boundary condition accounts for the presence of a boundary layer in the vicinity of the sphere surface, for $\sigma_C < r < \bar{\sigma}_C$, where the continuum diffusion description breaks down.

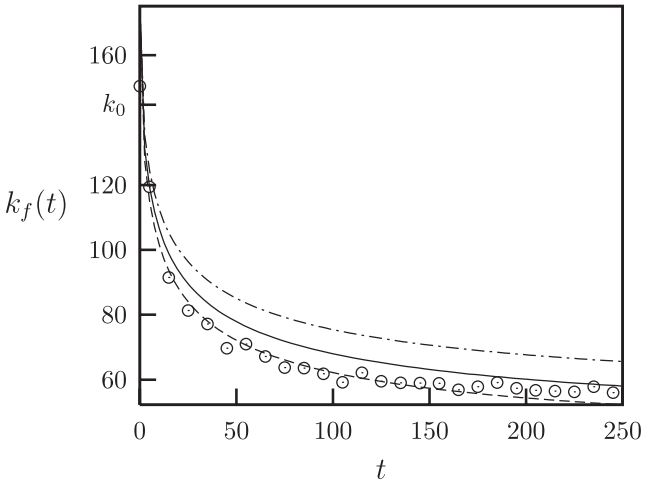

Figure 4. Plot of the time dependent rate constant $k_f(t)$ versus time for $\sigma_C = 10, \bar{\sigma}_C = 11$ and $\phi = 0.15$. The dot–dashed line is the prediction given by equation (9) when no obstacles are present. The solid line again uses equation (9) but with the theoretical value of $D(\phi)$ given in equation (4), while the dashed line uses the simulation value of $D(\phi)$ in the presence of the catalytic sphere given in figure 1.

When the diffusion equation is solved subject to this boundary condition the time dependent rate coefficient is given by [42]

$$k_f(t) = \frac{k_{0f}k_D}{k_{0f}+k_D} + \frac{k_{0f}^2}{k_{0f}+k_D}\exp\left[\left(1+\frac{k_{0f}}{k_D}\right)^2\frac{D}{\bar{\sigma}_C^2}t\right]\mathrm{erfc}\left[\left(1+\frac{k_{0f}}{k_D}\right)\left(\frac{Dt}{\bar{\sigma}_C^2}\right)^{1/2}\right]. \tag{9}$$

Here $k_D = 4\pi\bar{\sigma}_C D$ is the rate constant for a diffusion-controlled reaction for a perfectly absorbing sphere [39, 40]. The rate constant k_{0f} that characterizes the reactive process in the boundary layer may be taken to be that given for binary collisions of A with the catalytic sphere. For bounce-back collision dynamics of the A species with the catalytic sphere C, we have

$$k_{0f} = p_R\sigma_C^2\left(\frac{8\pi k_B T}{m}\right)^{1/2}. \tag{10}$$

The time dependent rate coefficient tends to its asymptotic constant value $k_f = k_{0f}k_D/(k_{0f}+k_D)$ as

$$k_f(t) \sim k_f\left(1+\frac{k_{0f}}{k_{0f}+k_D}\frac{\bar{\sigma}_C}{(\pi Dt)^{1/2}}\right). \tag{11}$$

An example of the evolution of the time dependent rate coefficient to its asymptotic value is plotted in figure 4 (open circles). There is a rapid fall from the initial value k_{0f}, followed by a much slower approach to the constant asymptotic value k_f. In this figure we also compare the simulation results with three simple analytical approximations based on equation (9) which neglect the presence of obstacles or include their effect through the volume fraction dependence of the diffusion coefficient. The best fit to the data is obtained when the simulation value of $D(\phi)$ which accounts for the presence of the large catalytic sphere is used in conjunction with equation (9).

Another non-trivial effect of crowding appears in the value of the intrinsic rate constant k_{0f}. In the simple model for this rate constant based on independent binary collisions with the

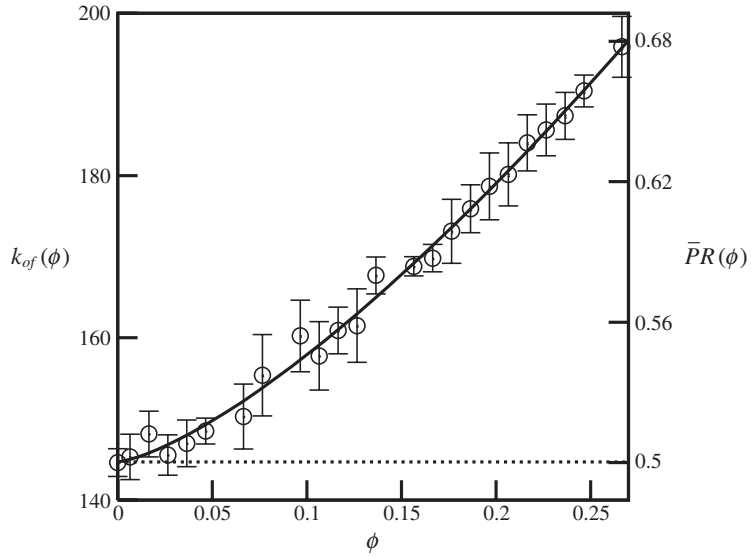

Figure 5. Simulated rate constant $k_{0f}(\phi)$ as a function of volume fraction ϕ. The solid line plots the change in the reaction probability $\bar{p}_{\mathrm{R}}(\phi)$ due to obstacles in the vicinity of the catalytic sphere surface. The horizontal dotted line is the binary collision estimate of k_{0f} given by equation (10).

catalytic sphere surface (equation (10)), k_{0f} is independent of the obstacle volume fraction. If this quantity is computed from the initial decay of the A number density field that occurs in one time unit, we find that k_{0f} depends on the volume fraction. This dependence is shown in figure 5 where $k_{0f}(\phi)$ is plotted versus ϕ. This increase is due to a number of factors that have their origin in the obstacle distribution in the vicinity of the catalytic sphere surface. Due to the presence of obstacles, a reactive small particle could collide with the catalytic sphere more than once in a unit time. In addition, due to the obstacle structural ordering near the sphere for high volume fractions shown in figure 3, the local density of A particles is higher near the catalytic sphere surface than in the bulk of the system. This is the larger of these two contributing effects. Figure 6 plots the initial local density of A particles $n_A(r)$ versus r, the radial distance from the catalytic sphere (solid lines). The variations in the initial A density track the changes in the local volume fraction in figure 3. Since the initial rate computed in a unit time interval is determined from equation (6) by dividing the initial rate of change of the A density by the mean density of A, a rate constant larger than that predicted by equation (10) will be obtained. For later times, as a result of the reaction $A + C \rightarrow B + C$, there is a depletion of A in the neighbourhood of the C as expected and this is shown in the figure (dotted lines).

These effects can be viewed as an increase the reaction probability p_{R} that depends on the volume fraction of obstacles[5]. If we write $k_{0f}(\phi) = \bar{p}_{\mathrm{R}}(\phi)\sigma_C^2(8\pi k_{\mathrm{B}}T/m)^{1/2}$ we can examine the magnitude of this enhancement. The effective reaction probability $\bar{p}_{\mathrm{R}}(\phi)$ is plotted in figure 5 (right ordinate axis). The volume fraction dependent reaction probability is well approximated by the form $\bar{p}_{\mathrm{R}}(\phi) = p_{\mathrm{R}}(1 + c\phi^{\alpha})$, where the exponent $\alpha \approx 1.4 \pm 0.1$ and $c \approx 2.0 \pm 0.08$. This functional form, with the same values of α and c, also fits the rate

[5] The effect of increased A density at the catalytic sphere surface for large ϕ on the value of k_{0f} is similar to that for high density hard sphere systems where the Enskog value of the intrinsic rate constant replaces the Boltzmann value [42]. Here, however, the effect arises from the high density of the obstacles. In the absence of obstacles the small molecules satisfy an ideal equation of state. The structure in the local density is induced by the structural ordering of the obstacles for large ϕ.

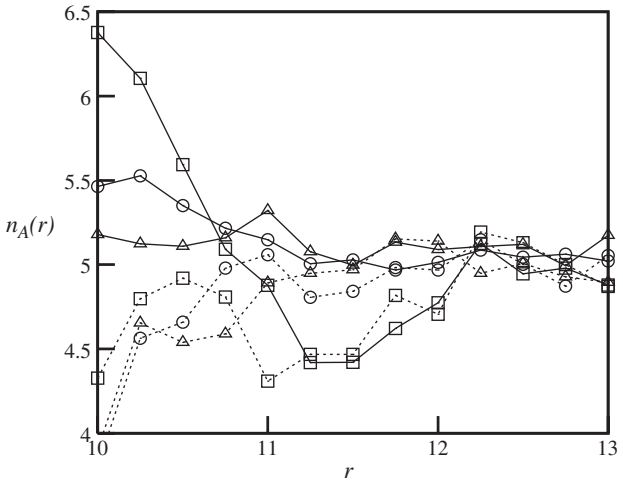

Figure 6. Radial density field of species A, $n_A(r)$, as a function of the distance, r, to the centre of catalytic sphere at initial time (solid lines), and after 10 simulation time steps (dotted lines). Squares, circles and triangles denote the radial density field for $\phi = 0.30$, 0.15, and 0.05 respectively.

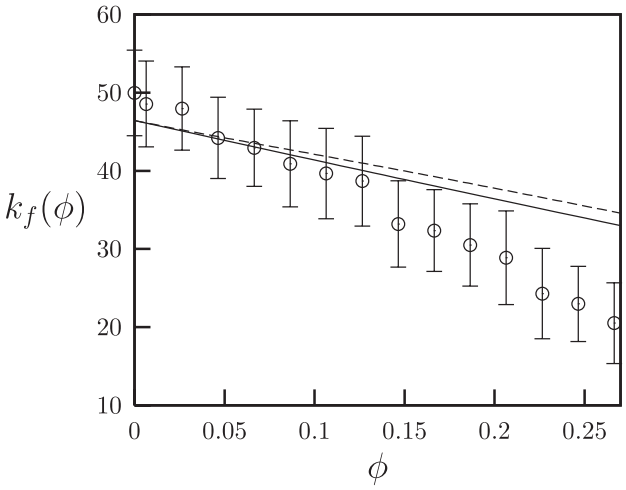

Figure 7. Plot of the asymptotic value of $k_f(\phi)$ as a function of the obstacle volume fraction ϕ. The solid and dashed lines are the theoretical estimates discussed in the text.

coefficient data for catalytic spheres with radii $r_C = 1, 2$ and 5, as well as the results for $r_C = 10$ presented in figure 5.

The volume fraction dependence of the asymptotic value of the rate constant $k_f(\phi)$ is shown in figure 7. These results were obtained from a linear regression of the data for $k_f(t)$ using the first 200 time steps of the simulation in order to avoid effects due to the use of periodic boundary conditions on the system. As expected, the rate constant decreases with increasing ϕ, consistent with the fact that the diffusion coefficient decreases as the obstacle volume fraction increases. Equation (9) predicts that the asymptotic rate constant is given by

$$k_f(\phi) = \frac{k_{0f}(\phi)k_D(\phi)}{k_{0f}(\phi) + k_D(\phi)}, \tag{12}$$

where the ϕ dependence of $k_{0f}(\phi)$ was discussed earlier and the ϕ dependence of $k_D(\phi)$ arises from $D(\phi)$ in this quantity. Using the simulation values of $k_{0f}(\phi)$ and $k_D(\phi)$ determined above, we plot this estimate for $k_f(\phi)$ in figure 7 as the solid line. The dashed line is a similar estimate but using equation (10) for k_{0f}; the ϕ dependence of k_{0f} has only a small effect on the overall rate constant since k_D dominates. These expressions are able to fit the data for small volume fractions but they are not quantitatively accurate for larger volume fractions.

While we have focused on the ϕ dependence of the rate constant for a single catalytic sphere (or equivalently a dilute suspension of catalytic spheres) in a field of stationary obstacles with high volume fraction, the investigation of the ϕ dependence of the rate constant for a dense suspension of catalytic spheres is a problem that has been studied often [36, 38, 43–48]. It is known that the rate constant is a non-analytic function of the volume fraction whose leading order behaviour is given by [38, 43]

$$k_f(\phi) = k_f\left[1 + \left(\frac{(k_{0f})^3}{(k_{0f}+k_D)^3}3\phi\right)^{1/2} + \cdots\right]. \tag{13}$$

The volume fraction dependence of the rate constant for a random distribution of catalytic spheres has been simulated using MPC dynamics [36]. In this case the rate constant increases with increasing volume fraction. This suggests that it is interesting to consider the effects of inert obstacle crowding on systems with high densities of catalytic molecules.

5. Conclusion

Diffusive and reactive rate processes involving small molecules occur at different rates in crowded and simple environments. While some of the qualitative effects due to crowding are easily anticipated—for example, the reduction of the diffusion coefficient as the volume fraction of obstacles increases—theories that quantitatively predict the magnitudes of the changes in transport properties as a function of the degree of crowding are largely still lacking. Even for the simple, highly idealized situations considered in this paper, there are few known results against which theories can be tested and trends due to crowding can be explored.

These factors have motivated our simulations of transport in crowded systems. While is possible to study these effects using full molecular dynamics methods, it would require a very large computational effort to carry out such simulations on the systems investigated in this paper. In our systems with volume $V = (50)^3$ and a large volume fraction $\phi = 0.3$ of obstacles, there are approximately 10^4 obstacles and 2×10^5 small molecules. For systems with $V = (100)^3$ these numbers are eight times larger. It is a lengthy task to carry out a full molecular dynamics study on systems of this size for the long times needed to determine the rate constant. The use of the mesoscopic multiparticle collision model has allowed us to compute the diffusion and reaction rate transport coefficients for various degrees of crowding in an efficient manner. Our simulation results can be used to test theoretical models and have yielded insight into the effects of crowding on the transport properties of small molecules.

For the diffusion of small molecules in a random distribution of identical spherical obstacles, the theoretical expression for $D(\phi)$ in equation (4) is able to quantitatively describe the simulation results. However, the presence a large catalytic sphere among the array of obstacles leads to quantitative changes in the volume fraction dependence of the diffusion coefficient. These changes probably arise from obstacle density inhomogeneities in the vicinity of the catalytic sphere surface.

The rate constant has contributions that arise from both reaction-limited events involving molecules near the catalytic sphere surface and a diffusion-limited events that depend on how molecules diffuse from the bulk to the catalytic sphere surface. The reduction of the reaction

rate as ϕ increases can be attributed to the decrease of $D(\phi)$ with ϕ since the diffusion-limited contribution to the rate constant is $k_D(\phi) = 4\pi\bar{\sigma}_C D(\phi)$. The reaction-limited rate constant also depends on ϕ due to obstacle structural ordering near the catalytic sphere. The situation is different if there are many catalytic spheres since the rate constant increases with increase in the volume fraction of catalytic spheres. Theoretical models that accurately describe the dependence of $D(\phi)$ and $k_f(\phi)$ for high volume fractions of obstacles and catalytic spheres remain to be constructed.

In this paper we focused on small molecule dynamics in crowded environments. Even this simple case can provide useful information to help understand the nature of the dynamics of small molecules in crowded environments like the cell. The techniques introduced here can be extended to allow for obstacles of various sizes, dynamics of the obstacles and studies of large molecule dynamics among obstacles.

Acknowledgments

This work was supported in part by a grant from the Natural Sciences and Engineering Research Council of Canada, in part by the grant 04-005-01 from the Decanato de Investigación of Universidad Nacional Experimental del Táchira, and in part by the grant I-886-05-02-A from Consejo de Desarrollo Científico Humanístico y Tecnológico of Universidad de Los Andes.

References

[1] Goodsell D S 1991 *Trends Biochem. Sci.* **16** 203
[2] Fulton A B 1982 *Cell* **30** 345
[3] Record T M Jr, Courtenay E S, Caley S and Guttman S J 1998 *Trends Biochem. Sci.* **23** 190
[4] Laurent T C 1995 *Biophys. Chem.* **57** 7
[5] Zimmerman S P and Minton A P 1993 *Annu. Rev. Biophys. Struct.* **22** 27
[6] Minton A P 2001 *J. Biol. Chem.* **276** 10577
[7] Luby-Phelps K, Castle P E, Taylor D L and Lanni F 1987 *Proc. Natl Acad. Sci. USA* **84** 4910
[8] Gersohn N D, Porter K R and Trus B L 1985 *Proc. Natl Acad. Sci. USA* **82** 5030
[9] Schnell S and Turner T E 2004 *Prog. Biophys. Mol. Biol.* **85** 235
[10] Hall D and Minton A P 2003 *Biochim. Biophys. Acta* **1649** 127
[11] Eggers D K and Valentine J S 2001 *Protein Sci.* **10** 250
[12] van den Berg B, Ellis R J and Dobson C M 1999 *EMBO J.* **18** 6927
[13] Ellis R J and Hartl F-U 1999 *Curr. Opin. Struct. Biol.* **9** 102
[14] Zimmerman S B and Trach S O 1991 *J. Mol. Biol.* **222** 599
[15] Zhou H-X 2004 *J. Mol. Recognit.* **17** 368
[16] Malevanets A and Kapral R 1999 *J. Chem. Phys.* **110** 8605
[17] Malevanets A and Kapral R 2000 *J. Chem. Phys.* **112** 7260
[18] Malevanets A and Kapral R 2003 Mesoscopic multi-particle collision model for fluid flow and molecular dynamics *Novel Methods in Soft Matter Simulations* ed M Karttunen, I Vattulainen and A Lukkarinen (Berlin: Springer) p 113
[19] Ihle T and Kroll D M 2001 *Phys. Rev.* E **63** 020201
[20] Lamura A, Gompper G, Ihle T and Kroll D M 2001 *Europhys. Lett.* **56** 768
[21] Lamura A, Gompper G, Ihle T and Kroll D M 2001 *Europhys. Lett.* **56** 319
[22] Kikuchi N, Pooley C M, Ryder J F and Yeomans J M 2003 *J. Chem. Phys.* **119** 6388
[23] Lee S H and Kapral R 2004 *J. Chem. Phys.* **121** 11163
[24] Lee S H and Kapral R 2005 *J. Chem. Phys.* **122** 214916
[25] Malevanets A and Yeomans J M 2000 *Europhys. Lett.* **52** 231
[26] Ripoll M, Mussawisade K, Winkler R G and Gompper G 2004 *Europhys. Lett.* **68** 106
[27] Winkler R G, Mussawisade K, Ripoll M and Gompper G 2004 *J. Phys.: Condens. Matter* **16** S3941
[28] Winkler R G, Ripoll M, Mussawisade K and Gompper G 2005 *Comput. Phys. Commun.* **169** 326
[29] Mussawisade K, Ripoll M, Winkler R G and Gompper G 2005 *J. Chem. Phys.* **123** 144905
[30] Malevanets A and Yeomans J 2000 *Europhys. Lett.* **52** 231

[31] Ali I, Marenduzzo D and Yeomans J M 2004 *J. Chem. Phys.* **121** 8635
[32] Kikuchi N, Gent A and Yeomans J M 2002 *Eur. Phys. J.* E **9** 63
[33] Hashimoto Y, Chen Y and Ohashi H 2000 *Comput. Phys. Commun.* **129** 56
[34] Inoue Y, Chen Y and Ohashi H 2002 *Colloids Surf.* A **201** 297
[35] Sakai T, Chen Y and Ohashi H 2002 *Phys. Rev.* E **65** 031503
[36] Tucci K and Kapral R 2004 *J. Chem. Phys.* **120** 8262
[37] Tucci K and Kapral R 2005 *J. Phys. Chem.* B **109** 21300
[38] Lebenhaft J and Kapral R 1979 *J. Stat. Phys.* **20** 25
[39] von Smoluchowski M 1915 *Ann. Phys.* **48** 1003
von Smoluchowski M 1916 *Phys. Z.* **17** 557
[40] von Smoluchowski M 1917 *Z. Phys. Chem.* **92** 129
[41] Collins F C and Kimball G E 1949 *J. Colloid Sci.* **4** 425
[42] Kapral R 1981 *Adv. Chem. Phys.* **48** 71
[43] Felderhof B U and Deutch J M 1976 *J. Chem. Phys.* **64** 4551
[44] Felderhof B U, Deutch J M and Titulaer U M 1982 *J. Chem. Phys.* **76** 4178
[45] Felderhof B U and Jones R B 1995 *J. Chem. Phys.* **103** 10201
[46] Gopich I V, Kipriyanov A A and Doktorov A B 1999 *J. Chem. Phys.* **110** 10888
[47] Felderhof B U and Jones R B 1999 *J. Chem. Phys.* **111** 4205
[48] Gopich I V, Berezhkovskii A M and Szabo A 2002 *J. Chem. Phys.* **117** 2987